Supplement Value of Magnetic Resonance Imaging in Small Hepatic Lesion (≤ 20 mm) Detected on Routine Computed Tomography

Sith Phongkitkarun MD*,
Tichakorn Srianujata MD*, Janjira Jatchavala MD*

** Department of Radiology, Faculty of Medicine, Ramathibodi Hospital, Mahidol University, Bangkok, Thailand*

Objective: *To determine the supplemental MRI value in characterization of small hepatic lesions (≤ 20 mm) indetermined by routine CT scan.*
Material and Method: *This was a retrospective study. Sixty-four patients with 81 indeterminate small hepatic lesions on the CT scan were included in this study. Two radiologists simultaneously evaluated the CT scan, followed by MRI. Patient history, imaging record, and final diagnosis were blinded. Final diagnoses were made by interpretation of all medical data and defined these lesions as benign or malignancy by using either histology or follow-up imaging combined with laboratory data.*
Results: *In 64 patients, 62 lesions (76.5%) of 81 indeterminate lesions were benign, whereas 19 lesions (23.5%) were malignant. MRI interpreted 55 lesions as benign, 17 lesions as malignant, and 9 as indeterminate lesions. If the indeterminate lesions were assumed as benign lesions, sensitivity, specificity, positive predictive value (PPV), and negative predictive value (NPV), are 68.4%, 93.6%, 76.5%, and 90.6%, respectively.*
Conclusion: *MRI can supplement CT scan in characterization of small hepatic lesion with high specificity and accuracy.*

Keywords: *Liver diseases, Liver neoplasms, Magnetic resonance imaging, Tomography, X-ray computed*

J Med Assoc Thai 2009; 92 (5): 677-86
Full text. e-Journal: *http://www.mat.or.th/journal*

Focal hepatic lesion is a common problem in liver disease. The distinction between benign and malignant lesions is clinically important because surgical resection is the most effective treatment of small malignant lesions whereas it is not necessary for the benign lesions. For example, the 5-year survival rate in patients with small HCC who undergo surgical resection is over 80%. Therefore, early detection of small HCC is highly critical for the patient outcome[1-3].

Numerous imaging modalities have currently been used for radiological detection and characterization of liver tumors[1,4]. Computed tomography (CT) is commonly used to confirm and characterize a suspicious nodule because of its widespread availability and rapid acquisition time. Recent advances in the CT scanner with multislice technology up to 64 slices and extremely short acquisition time have more facilitated to detect small hepatic lesions (≤ 20 mm), even though characterization of those lesions is still a problem[2-6].

Magnetic resonance imaging (MRI) is frequently used as a problem-solving modality for the evaluation of lesions considered indeterminate on other imaging modalities[3,5-8]. It offers good contrast resolution and diagnostic sensitivity over 90%[3,9]. However, the main difficulty is not in diagnosis of large lesions, but rather small lesions (≤ 20 mm), particularly in patients with a history of cancer or underlying liver disease such as cirrhosis that may carry an increased risk for cancer[3,8]. Moreover, due to the

Correspondence to: Phongkitkarun S, Department of Radiology, Faculty of Medicine, Ramathibodi Hospital, Mahidol University, Rama VI Rd, Ratchathewi, Bangkok 10400, Thailand. Phone: 0-2201-1260, Fax: 0-2201-1297, E-mail: rasih@mahidol.ac.th

limited availability of MRI to only some institutes, its high cost and the many previous studies showing much less accurate for lesions less than 2 cm in diameter, it is still controversial as to the benefit of MRI in the characterization of the small hepatic lesions[2,3,6,9-10].

The purpose of the present study was to determine the supplemental MRI value in characterization of small hepatic lesions (≤ 20 mm) those undetermined by routine CT scan.

Material and Method

Patients

This was a retrospective study approved by our institutional research ethics committee. The authors reviewed their database from Advance Diagnostic Imaging and Image Guided Minimal Invasive Therapy Center (AIMC), Ramathibodi Hospital, for individuals who underwent liver MR imaging between January 2001 and March 2005 for the evaluation of small hepatic lesions (≤ 20 mm) that had previously been visualized on routinely performed CT and had been considered indeterminate. All lesions must have a final diagnosis as benign or malignant by histology or follow-up imaging. Exclusion criteria were cases with known diagnosis of liver lesion at the time of first CT and those with either loss of imaging material or medical record.

Seventy-one patients were eligible. Seven of them were excluded for the following reason: five had been confidently characterized the lesions from the first CT, and two had no definite lesion seen on the first CT. There were 64 patients included in the present study with total 81 nodules. The group included 31 male and 33 female patients, whose ages ranged from 32 to 78 years (mean age, 58 years). Fifty-one patients had one indeterminate lesion, nine patients had two indeterminate lesions, and four patients had three indeterminate lesions. Thirty-eight patients had underlying liver cirrhosis caused by chronic hepatitis B viral infection (n = 22), hepatitis C viral infection (n = 14), and alcoholic hepatitis (n = 2). Nineteen patients had a known diagnosis of primary malignancy such as breast cancer (n = 4), sigmoid colon cancer (n = 4), hepatocellular carcinoma (n = 3), bladder cancer (n = 2), ovarian cancer (n = 2), rectal cancer (n = 1), gastric cancer (n = 1), lung cancer (n = 1), and non-Hodgkin lymphoma (n = 1).

All patients underwent CT, followed by MR examination with timing between two examinations ranged from 4 to 93 days; mean timing was 30 days.

Imaging techniques

CT technique

All CT scans were performed with 4-slice mutidetector CT (Lightspeed plus; General Electric Medical System, Milwaukee, WI). After obtaining the unenhanced images through the liver with 10-mm collimation, arterial phase and portal venous phase images were acquired with a collimation of 2.5-3.75 mm. A total of 2 ml/kg of iopromide (Ultravist; Schering, Germany), iobitridol (Xenetic; Guerbet, Germany) or iohexol (Omnipaque; Amersham, China) was administered intravenously by using a mechanical power injector at a rate of 2-2.5 ml/sec. The scanning was begun 25-30 seconds after the start of the injection.

MR imaging technique

In fifty-seven patients, MR imaging was performed on a 1.5-T unit (General Electric Medical Systems, Milwaukee, WI) with high-performance gradients and a body phased-array coil. In seven patients, MR imaging was performed on a 3.0-T unit (Philips Medical Systems, Best, The Netherlands). All patients underwent axial T1- and T2-weighted MR imaging. T1-weighted imaging included at least one of the following sequences: conventional spin-echo imaging (TR range/TE range, 400-600/10-20); in-phase spoiled gradient-echo imaging (TR range/TE, 170-240/4.7; flip angle 90°); and opposed-phase spoiled gradient-echo imaging (TR range/TE, 170-240/2.2; flip angle 90°). T2-weighted imaging included fast spin-echo imaging (TR range/TE range, 2000-4000/60-100), gradient T2-weighted imaging (TR range/TE, 400-800/20, flip angle 25°) and single-shot fast spin-echo imaging (TR/TE_{eff}, infinite/80). The imaging matrix used was 256 x 160-192 pixels. The section thickness was 6-8 mm with an intersection gap of 1-2 mm.

Dynamic contrast-enhanced MR imaging of the liver was performed in all patients before and after intravenous bolus administration of 0.2 ml/kg of gadopentetate dimeglumine (Magnevist; Schering, Germany) given approximately at a rate of 1.5 ml/sec by hand, followed by 10-15 ml of saline flush. Dynamic imaging was performed with axial volumetric fat-suppressed spoiled gradient-echo breath-hold imaging (TR/TE, 8.0/4.2; flip angle 12°). After unenhanced imaging, arterial phase images were obtained during 15-20 sec after the start of IV bolus administration. Second and third sets of images were obtained after allowing the patient to take another breath, approximately 45 sec and 90 sec, respectively. The imaging matrix was 256 x 160-192 pixels. The section thickness

was 8 mm with zero intersection gap. Then axial T1-weighted image (TR range/TE range, 400-600/10-20) with fat suppression was performed at 5 minutes after IV contrast administration.

Superparamagnetic iron oxide (SPIO) agent was used in 12 patients with 15 lesions. A total 1.4 ml of SPIO (Resovist; Schering, Germany) was intravenously administrated to the patient by hand, followed by 10-15 cc of saline flush. Dynamic SPIO-enhanced MR imaging was performed with the same technique as dynamic gadolinium-enhanced image. Then 10-minute delayed image was performed with axial T2-weighted gradient-echo image (TR range/TE, 400-800/20, flip angle 25°) and T2-weighted image (TR range/TE range, 2000-4000/60-100) with fat suppression.

Imaging analysis

Two participants, one a board certified gastro-intestinal radiologists (S.P. and J.J.), simultaneously evaluated CT scan, followed by MR imaging. The reviewers were unaware of the patient's history, imaging record and final diagnosis. The MR imaging diagnoses were made in consensus lesion-by-lesion, as benign, malignant or indetermination.

Lesion confirmation

The final diagnoses were made by interpretation of all medical data and defined these nodules as benign or malignant by using either histology or follow-up imaging combined with laboratory data. Criteria for diagnosis of malignancy by follow-up imaging were a significant increase in size (30% increased size within one year[5]) or newly detected early arterial-phase enhancement of previously seen hepatic lesion.

Final diagnosis of 81 lesions were confirmed by histology in 16 lesions (six by imaging guided percutaneous biopsy, five by segmentectomy, two by non-anatomical wedge resection, two by imaging guided aspiration, and one by open surgical biopsy). The other lesions (n = 65) were confirmed on the basis of a combination of clinical and laboratory data and serial follow-up imaging, using MRI (n = 26), CT (n = 23) and sonography (n = 16).

Of the 81 lesions, nineteen were confirmed as malignancy and sixty-two as benign. The malignant lesions consisted of 14 primary hepatocellular carcinoma and 5 metastases, known primary malignancy: lung cancer (n = 3), sigmoid colon cancer (n = 1), and gastric cancer (n = 1). The 62 benign lesions consisted of hemangioma (n = 17), regenerative nodule (n = 16), hepatic cyst (n = 12), focal nodular hyperplasia (n = 4), perfusion abnormality (n = 3), focal fatty infiltration (n = 1), fibrotic tissue (n = 1), pseudolesion (n = 1), and non-specific lesion (n = 7).

Statistical analysis

All data collected were placed into Epidata version 3.02 for analysis by using STATA, version 9.0 (STATA, College station, TX). The characteristics of the diagnostic test including sensitivity, specificity, positive predictive value, negative predictive value, and accuracy with 95% confidence interval were calculated per lesion and per patient. To evaluate the effect of those indeterminate lesions interpreted by MRI on the diagnostic performance, the authors separated the data using two different thresholds for assigning those lesions as benign or malignant and subsequently calculated cumulative sensitivity, specificity and corresponding positive and negative predictive values.

Threshold 1 defined those indeterminate lesions as benign

Threshold 2 defined those indeterminate lesions as malignant

Descriptive statistical analysis of those indeterminate lesions interpreted by MRI was also performed.

Results

In 64 patients, there were 81 small hepatic lesions (≤ 20 mm), which were indeterminate on CT scan; 62 lesions (76.5%) of 81 lesions were benign by histology or follow-up imaging, whereas 19 lesions (23.5%) were malignant (Table 1). All patients underwent MRI; 55 lesions were interpreted as benign, 17 as malignant, and 9 as indeterminate lesions. Timing between first CT scan and MRI ranged from 4-93 days (mean, 30 days). The size of the lesions ranged from 3 to 20 mm (mean, 11 mm) at the first CT scan. Only one lesion, which was proven as metastatic leiomyosarcoma from primary gastric cancer, became significantly larger in the following MRI, measuring from 11 to 20 mm in size. The others were stable in size.

The diagnostic performance of MR imaging in both threshold 1 and 2, lesion basis and patient basis are shown in Tables 2 and 3, respectively. The diagnostic value included sensitivity, specificity, positive predictive value (PPV), negative predictive value (NPV), area under the receiver operating characteristic (ROC) curve (A_z value), standard error and the accuracy. Fig. 1 and 2 show ROC curves of

Table 1. MR imaging diagnosis of 81 small hepatic lesions in 64 patients

Lesions	No. of lesions interpreted as benign	No. of lesions interpreted as indetermination	No. of lesions interpreted as malignant	Total
Benign				
Hemangioma	13	2	2	17
Regenerative nodule	12	4	0	16
Cyst	12	0	0	12
Focal nodular hyperplasia	3	0	1	4
Focal fatty infiltration	1	0	0	1
Perfusion abnormality	3	0	0	3
Fibrotic tissue	1	0	0	1
Hypervascular pseudolesion	0	0	1	1
Not specified	7	0	0	7
Total	52	6	4	62
Malignant				
Primary hepatocellular carcinoma	3	3	8	14
Metastasis				
Colon cancer	0	0	1	1
Gastric cancer	0	0	1	1
Lung cancer	0	0	3	3
Total	3	3	13	19

Table 2. Diagnostic performance of MR imaging in small hepatic lesion, per lesion

Test	Sensitivity (%) (95% CI)	Specificity (%) (95% CI)	PPV (%) (95% CI)	NPV (%) (95% CI)	Accuracy (%)	ROC area (standard error)
MRI threshold 1	68.4 (58-79)	93.6 (88-99)	76.5 (67-86)	90.6 (84-97)	87.7	0.81 (0.06)
MRI threshold 2	84.2 (76-92)	83.9 (76-92)	61.5 (51-72)	94.6 (90-99)	84.0	0.84 (0.05)

p-value = 0.52

Table 3. Diagnostic performance of MR imaging in small hepatic lesion, per patient

Test	Sensitivity (%) (95% CI)	Specificity (%) (95% CI)	PPV (%) (95% CI)	NPV (%) (95% CI)	Accuracy (%)	ROC area (standard error)
MRI threshold 1	64.3 (53-76)	94.0 (88-100)	75.0 (64-86)	90.4 (83-98)	87.5	0.79 (0.07)
MRI threshold 2	78.6 (69-89)	84.0 (75-93)	57.9 (46-70)	93.3 (87-99)	82.8	0.81 (0.06)

p-value = 0.69

diagnostic performance of MR imaging, per lesion and per patient, respectively. There was no statistical significant difference in A_z value between threshold 1 and 2 in both groups.

There were four benign lesions in four patients that were misinterpreted as malignancy by MR imaging, compose of two hemangiomas, one focal nodular hyperplasia (FNH), and one hypervascular pseudolesion. Two hemangiomas were misinterpreted as malignant due to their atypical appearances, which showed isointense on T2W image with continuous rim enhancement in arterial phase and isointense in portal venous phase. One FNH also displayed atypical appearance as shown in Fig. 3, as well as one

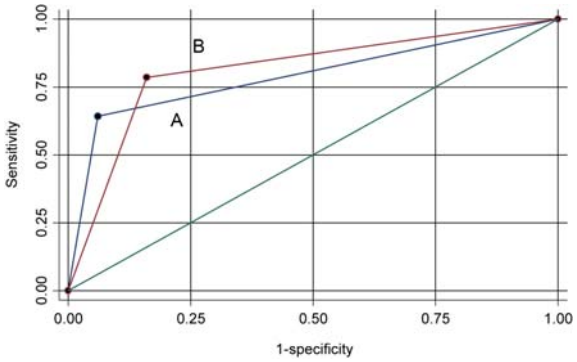

Fig. 1 Receiver operating characteristic (ROC) curves show the diagnostic performance of MR imaging, per lesion. Curve A represents ROC curve of threshold 1, with area under curve (and standard error) of 0.81 (0.06), whereas curve B represents ROC curve of threshold 2, with area under the curve (and standard error) of 0.84 (0.05)

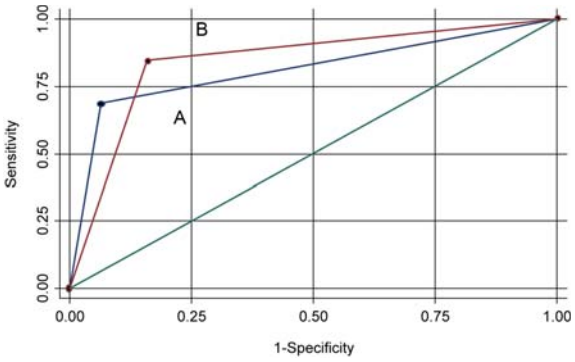

Fig. 2 Receiver operating characteristic (ROC) curves show the diagnostic performance of MR imaging, per patient. Curve A represents ROC curve of threshold 1, with area under curve (and standard error) of 0.79 (0.07), whereas curve B represents ROC curve of threshold 2, with area under the curve (and standard error) of 0.81 (0.06)

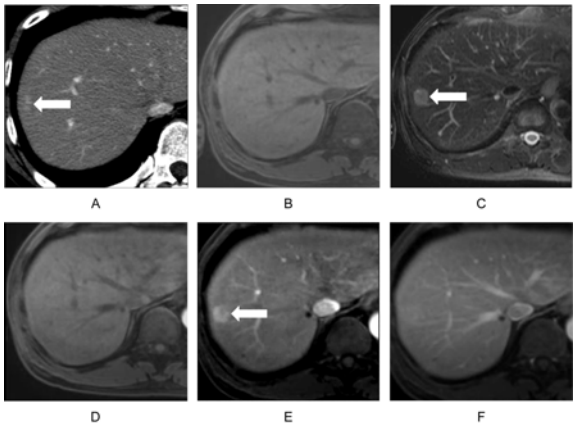

Fig. 3 A 64-year-old man with history of cirrhosis caused by chronic hepatitis B viral infection. A 9-mm nodule at hepatic segment 8 was interpreted as hepatocellular carcinoma by MR imaging. Open liver biopsy was performed at 1 month after MR imaging; histology revealed focal nodular hyperplasia. Serial follow-up MR imaging for 1 year shows no significant change in size of the lesion (arrow in A, C and E)
A, Late arterial phase CT scan shows inhomogeneous enhancement area at hepatic segment 8
B and C, Conventional spin-echo T1-weighted MR image (B) at 10 days after CT scan shows isoosignal intensity of the same lesion with hypersignal intensity on fast spin-echo T2-weighted MR image (C)
D, E and F, Dynamic gadolinium enhanced T1-weighted spoiled gradient-echo MR images, the lesion shows isosignal intensity in arterial phase (D) with inhomogeneous enhancement in portal venous phase (E) and relatively contrast wash-out in equilibrium phase (F)

hypervascular pseudolesion that was atypically presented as HCC (Fig. 4).

Three of the malignant lesions in three patients were misinterpreted as benign lesions. All of them were proved as HCC. The imaging characteristics of the first lesion mimicked FNH, as shown in Fig. 5. The other two lesions showed no enhancement in all phases of dynamic gadolinium enhanced image, but the 15-month and 3-month follow-up imaging of these two lesions revealed early arterial enhancement.

Among nine indeterminate lesions in eight patients, seven (78%) were found in six cirrhotic livers, and two (22%) in non-cirrhotic livers; six were benign (2 of atypical hemangiomas and 4 of regenerative nodules) and three were malignancy (all are primary HCCs). Indeterminate lesions were found in six of 38 (16%) of cirrhotic patients. The details of the indeterminate lesions are summarized in Table 4. Fig. 6 and 7 are the examples of these lesions.

Discussion

In general, MRI is considered a problem-solving modality for characterization of focal liver lesions, which are indeterminate by CT, because of its unique ability to provide high intrinsic soft tissue contrast and the use of non-specific and specific contrast media[11]. The present study focused on lesions smaller than 2 cm, which were referred to MR imaging after the nature of the lesions could not be determined on CT and demonstrated that MRI has supplement value in characterization these indeterminate lesions with high specificity and accuracy.

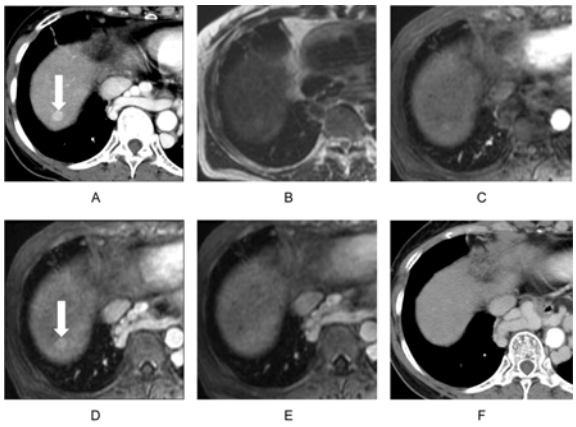

Fig. 4 A 70-year-old female with history of cirrhosis caused by chronic hepatitis C viral infection. A 10-mm nodule at hepatic segment 7 was interpreted as hepatocellular carcinoma by MR imaging (arrow in A and D)
A, Arterial phase CT scan shows homogeneous arterial enhancement nodule at hepatic segment 7
B, Fast spin-echo T2-weighted MR image at 2 months after CT scan shows hypersignal intensity
C, D and E, Dynamic gadolinium enhanced T1-weighted spoiled gradient-echo MR images, the lesion shows homogeneous enhancement in arterial (C) and portal venous phases (D) with relatively isosignal intensity in equilibrium phase (E)
F, Follow-up CT scan at 11 months after MR imaging shows disappearance of the previously seen hypervascular lesion. The lesion was considered hypervascular pseudolesion

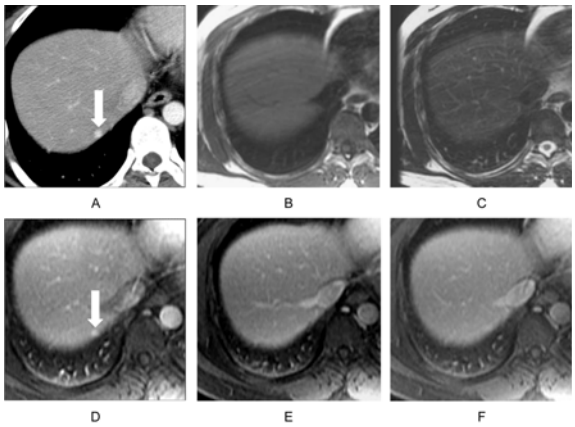

Fig. 5 A 32-year-old man with known hepatocellular carcinoma at left hepatic lobe, status post wedge resection for 2 years. His serial follow-up imaging shows a 6-mm nodule at hepatic segment 7 that was interpreted as focal nodular hyperplasia by MR imaging. Patient underwent non-anatomical wedge resection at 1 month after MR imaging and histology reveals hepatocellular carcinoma (arrow in A and D)
A, Arterial phase CT scan shows homogeneous arterial enhancement nodule at hepatic segment 7
B and C, Conventional spin-echo T1-weighted MR image (B) and fast spin-echo T2-weighted MR image (C) at 11 days after CT scan show isosignal intensity of the lesion
D, E and F, Dynamic gadolinium enhanced T1-weighted spoiled gradient-echo MR images, the lesion shows homogeneous enhancement on arterial phase (D) with isosignal intensity in portal venous (E) and equilibrium phases (F)

Table 4. Characteristics of indeterminate lesions interpreted by MR imaging

Pt. No.	Size (mm)	Underlying disease		MRI characteristic							Final diagnosis ****
		Cirrhosis	Primary CA	Signal intensity*		Dynamic gadolinium enhancement**				SPIO enhancement ***	
				T1-weighted	T2-weighted	Arterial	PVP	Equilibrium	Delayed		
1	13	Yes	No	Hypo	Hyper	Homo	Homo	Homo	Homo	NP	HCC
2	13	Yes	No	Hypo	Hyper	No	No	Rim	Rim	NP	HCC
3	8	Yes	No	Iso	Iso	Homo	Iso	Iso	Iso	NP	HCC
4	9	Yes	No	Iso	Iso	Hetero	Iso	Iso	Iso	Partial	RN
5	4	Yes	Yes	Hyper	Iso	No	No	No	No	NP	RN
6	12	Yes	No	Iso	Iso	Homo	Iso	Iso	Iso	NP	RN
6	8	Yes	No	Iso	Iso	Homo	Iso	Iso	Iso	NP	RN
7	5	No	Yes	Iso	Hyper	No	Homo	Homo	Homo	NP	Hem
8	12	No	Yes	Hypo	Hyper, R	Rim	Rim	Rim	Rim	No	Hem

* Hyper = hyperintense; Iso = isointense; Hypo = hypointense; Hyper, R = hyperintense rim
** Homo = diffuse homogeneous enhancement; Inhomo = diffuse inhomogeneous enhancement; Rim = peripheral rim enhancement; No = non-enhancement
*** NP = not performed; No = no uptake; Partial = partial uptake
**** HCC = hepatocellular carcinoma; RN = regenerative nodule; Hem = hemangioma

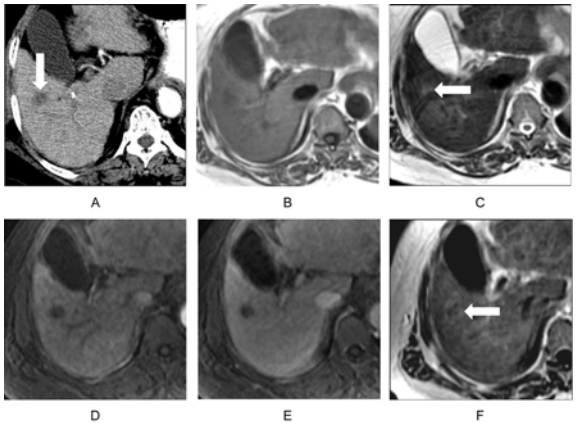

Fig. 6 A 68-year-old female with history of cirrhosis caused by chronic hepatitis B viral infection. A 13-mm nodule at hepatic segment 5 was interpreted as indetermination by MR imaging. CT guided liver biopsy was performed at 1 month after MR imaging and histology revealed hepatocellular carcinoma, clear cell type (arrow in A, C and F)
A, Arterial phase CT scan shows a hypodensity nodule without arterial enhancement
B and C, Conventional spin-echo T1-weighted MR image (B) shows hyposignal intensity of the same lesion with slightly hypersignal intensity on fast spin-echo T2-weighted MR image (C)
D, E and F, Dynamic gadolinium enhanced T1-weighted spoiled gradient-echo MR images, the lesion shows no enhancement in arterial (D) and portal venous phases (E). Peripheral rim enhancement is visualized in delayed phase image (F)

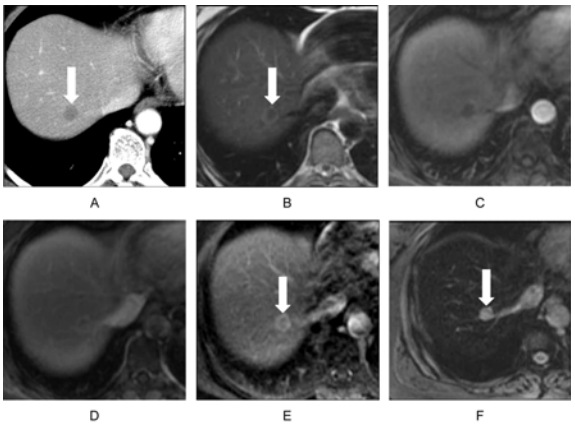

Fig. 7 A 57-year-old female with history of breast cancer. A 12-mm at hepatic segment 7 was interpreted as indetermination by MR imaging. A 6-month interval of serial follow-up sonogram for a year reveals no significant change in size of this lesion. It was considered atypical hemangioma (arrow in A, B, E and F)
A, Arterial phase CT scan shows a hypodensity nodule without arterial enhancement
B, Fast spin-echo T2-weighted MR image shows peripheral rim hypersignal intensity
C, D and E, Dynamic gadolinium enhanced T1-weighted spoiled gradient-echo MR images, the lesion shows peripheral nodular enhancement in arterial phase (C) with contiguous peripheral rim enhancement in equilibrium (D) and delayed phases (E)
F, Delayed phase T2-weighted gradient-echo image after 10 minutes of SPIO agent injection shows no contrast uptake of the lesion

Based on other MRI studies[8,14-15], most small hepatic lesions (≤ 20 mm) turn out to be benign entities. Therefore, the best diagnostic performance of MRI in this setting should be obtained by applying threshold 1, which regarded indeterminate lesions as benign. As expected, with a shift from threshold 1 to threshold 2, the sensitivity was increased and specificity was decreased. Based on threshold 1, high specificity was obtained and reflected MR imaging that is suitable for confirmation test rather than screening test. As well as giving the relatively low positive and high negative predictive values obtained by applying threshold 1, the authors found that MR imaging was more useful for excluding the possibility of malignancy than for detecting the presence of malignancy in this clinical setting. In agreement the findings of Mueller et al[8], who retrospectively studied effectiveness of MRI in characterization of 69 small (≤ 20 mm) hepatic lesions which were considered as indeterminate on previously CT. Expert interpretation revealed sensitivity of 73.6%, specificity of 100%, PPV of 100% and NPV of 94.9%. Noguchi et al[16] reported that dynamic MR imaging is recommended to improve detection and characterization of hypervascular hepatocellular carcinoma in addition to the use of dynamic helical CT with double phase imaging and showed sensitivity of 47% and PPV of 95% for MR imaging in characterization of lesion smaller than 2 cm. The presented results yield moderate sensitivity and high specificity of MR imaging in the indeterminate lesions on CT compared to the other studies.

As considered to the factor causing indetermination, false positive and false negative lesions interpreted by MR imaging in the present study, underlying cirrhosis was found in the majority of cases. In fact, characterization of small nodules is more difficult in patients with cirrhotic livers than in patients with normal livers because of the severely disturbed liver architecture and altered portal hemodynamics. Krinsky et al[17] prospectively assessed MR imaging

for the detection of HCC in cirrhotic liver by using explantation correlation in 71 patients. In their study, MRI detected HCC in only 33% (1 of 3 patients) of less than 10 mm nodules and 50% (6 of 12 patients) of 10-20 mm nodules. In addition, small HCC nodules (≤ 20 mm) are usually well differentiated. Classical HCCs are hyperintense on T2-weighted image whereas well-differentiated HCCs can be isointense or rarely hypointense[3,14], as one of the false negative lesions in the present study that showed isointense on T2-weighted image, MR imaging was misinterpreted as focal nodular hyperplasia. Ebara et al[18] showed that the signal intensity of HCC in T2-weighted images is related to the degree of histological differentiation. According to the study of Jeong et al[14] in small (≤ 20 mm) enhancing hepatic nodules seen on arterial phase MR imaging of the cirrhotic liver, the results revealed no significant correlation between diagnosis of small HCC and nodule signal intensity or contrast enhancement homogeneity on MR examination, whereas interval nodule growth is highly predictive of HCC with PPV of 100% and NPV of 98%. Therefore, small size and well-differentiated nature of early HCC account for the frequent failure to establish definite diagnosis using cross-sectional imaging and close follow-up serial imaging or tissue diagnosis often useful in this small lesion. MRI itself causes limitation of interpretation due to thick image section and many types of artifacts, particularly motion and respiratory artifacts.

On the other hand, being considered indeterminate, false positive and false negative lesions in non-cirrhotic livers, most of these lesions (80%) had been proven as atypical hemangiomas, which could manifest varying signal intensity on MR imaging.

Some factors caused limitation in the present study. First, inclusion of more than one lesion in some patients might have introduced a bias, resulting in better diagnostic performance. Second, the interval between CT scan and following MR imaging was one factor initiating reviewer bias, by changing or stabilizing tumor size between two studies. The authors have reduced this bias by blinded date during imaging interpretation. Therefore, there is one lesion in a patient with known primary cancer that is significantly larger in MR imaging causing more confidently interpreted as liver metastasis. Another one is a false negative lesion in cirrhotic patient that MR imaging interpreted as regenerative nodule although 15-months' follow-up CT shows early arterial enhancement, which can be possible timing for newly developed HCC. The method of lesion confirmation was one of the significant limitations, and only approximately 20% of the overall cases had histological diagnoses; the other 80% were confirmed by serial follow-up imaging that has more variation in diagnosis. Furthermore, among the total histological diagnoses, 50% was imaging guided percutaneous biopsy or aspiration, which can lead to misinterpretation because the entire pathologic specimens are needed for the accurate histological diagnoses.

Conclusion

MR imaging can supplement CT scan in characterization of small hepatic lesion with high specificity and accuracy because of its various imaging techniques and specific contrast media that are helpful for specified tissue characteristics of the lesion. However, the sensitivity for characterization of small hepatic lesion is still low to moderate.

Acknowledgement

The authors wish to thank Professor Dr. Amnuay Thithapandha from Division of Academic Affairs, Ramathibodi Hospital for his assistance in editing this paper and Dr. Sasivimol Rattanasiri from Clinical Epidemiology Unit, Research Center, Ramathibodi Hospital for statistical consultation.

References

1. Choi BI, Takayasu K, Han MC. Small hepatocellular carcinomas and associated nodular lesions of the liver: pathology, pathogenesis, and imaging findings. Am J Roentgenol 1993; 160: 1177-87.
2. Fung KT, Li FT, Raimondo ML, Maudgil D, Mancuso A, Tibballs JM, et al. Systematic review of radiological imaging for hepatocellular carcinoma in cirrhotic patients. Br J Radiol 2004; 77: 633-40.
3. Taouli B, Losada M, Holland A, Krinsky G. Magnetic resonance imaging of hepatocellular carcinoma. Gastroenterology 2004; 127: S144-S152.
4. Hussain SM, Zondervan PE, IJzermans JN, Schalm SW, de Man RA, Krestin GP. Benign versus malignant hepatic nodules: MR imaging findings with pathologic correlation. Radiographics 2002; 22: 1023-36.
5. O'Malley ME, Takayama Y, Sherman M. Outcome of small (10-20 mm) arterial phase-enhancing nodules seen on triphasic liver CT in patients with cirrhosis or chronic liver disease. Am J Gastroenterol 2005; 100: 1523-8.
6. Choi BI. The current status of imaging diagnosis

of hepatocellular carcinoma. Liver Transpl 2004; 10 (2 Suppl 1): S20-5.
7. Kim YK, Kim CS, Lee YH, Kwak HS, Lee JM. Comparison of superparamagnetic iron oxide-enhanced and gadobenate dimeglumine-enhanced dynamic MRI for detection of small hepatocellular carcinomas. Am J Roentgenol 2004; 182: 1217-23.
8. Mueller GC, Hussain HK, Carlos RC, Nghiem HV, Francis IR. Effectiveness of MR imaging in characterizing small hepatic lesions: routine versus expert interpretation. Am J Roentgenol 2003; 180: 673-80.
9. Federle MP. Use of radiologic techniques to screen for hepatocellular carcinoma. J Clin Gastroenterol 2002; 35 (5 Suppl 2): S92-100.
10. Holland AE, Hecht EM, Hahn WY, Kim DC, Babb JS, Lee VS, et al. Importance of small (< or = 20-mm) enhancing lesions seen only during the hepatic arterial phase at MR imaging of the cirrhotic liver: evaluation and comparison with whole explanted liver. Radiology 2005; 237: 938-44.
11. Hussain SM, Semelka RC. Hepatic imaging: comparison of modalities. Radiol Clin North Am 2005; 43: 929-47, ix.
12. Tello R, Fenlon HM, Gagliano T, deCarvalho VL, Yucel EK. Prediction rule for characterization of hepatic lesions revealed on MR imaging: estimation of malignancy. Am J Roentgenol 2001; 176: 879-84.
13. Bhartia B, Ward J, Guthrie JA, Robinson PJ. Hepatocellular carcinoma in cirrhotic livers: double-contrast thin-section MR imaging with pathologic correlation of explanted tissue. Am J Roentgenol 2003; 180: 577-84.
14. Jeong YY, Mitchell DG, Kamishima T. Small (< 20 mm) enhancing hepatic nodules seen on arterial phase MR imaging of the cirrhotic liver: clinical implications. Am J Roentgenol 2002; 178: 1327-34.
15. Shimizu A, Ito K, Koike S, Fujita T, Shimizu K, Matsunaga N. Cirrhosis or chronic hepatitis: evaluation of small (< or = 2-cm) early-enhancing hepatic lesions with serial contrast-enhanced dynamic MR imaging. Radiology 2003; 226: 550-5.
16. Noguchi Y, Murakami T, Kim T, Hori M, Osuga K, Kawata S, et al. Detection of hepatocellular carcinoma: comparison of dynamic MR imaging with dynamic double arterial phase helical CT. Am J Roentgenol 2003; 180: 455-60.
17. Krinsky GA, Lee VS, Theise ND, Weinreb JC, Rofsky NM, Diflo T, et al. Hepatocellular carcinoma and dysplastic nodules in patients with cirrhosis: prospective diagnosis with MR imaging and explantation correlation. Radiology 2001; 219: 445-54.
18. Ebara M, Fukuda H, Kojima Y, Morimoto N, Yoshikawa M, Sugiura N, et al. Small hepatocellular carcinoma: relationship of signal intensity to histopathologic findings and metal content of the tumor and surrounding hepatic parenchyma. Radiology 1999; 210: 81-8.

การตรวจด้วยเครื่องสร้างคลื่นแม่เหล็กไฟฟ้าช่วยในการวินิจฉัยก้อนขนาดเล็กของตับที่ตรวจพบจากเอกซเรย์คอมพิวเตอร์

สิทธิ์ พงษ์กิจการุณ, ทิชากร ศรีอนุชาต, จันทร์จิรา ชัชวาลา

วัตถุประสงค์: *จุดมุ่งหมายของการศึกษาครั้งนี้เพื่อศึกษาความเป็นไปได้ในการใช้คลื่นแม่เหล็กไฟฟ้า เพื่อวินิจฉัยก้อนขนาดเล็กที่ตับ (≤ 20 มม.) ที่ไม่สามารถให้การวินิจฉัยได้โดยเอกซเรย์คอมพิวเตอร์*

วัสดุและวิธีการ: *เป็นการศึกษาย้อนหลัง ประชากรที่นำมาศึกษาทั้งหมด 64 คน มีก้อนขนาดเล็กที่ตับที่ไม่สามารถให้การวินิจฉัยได้โดยเอกซเรย์คอมพิวเตอร์ทั้งหมด 81 ก้อน โดยให้รังสีแพทย์ 2 คนแปลผลภาพเอกซเรย์คอมพิวเตอร์ก่อน จากนั้นจึงแปลผลภาพคลื่นแม่เหล็กไฟฟ้า โดยไม่ให้ทราบข้อมูลอื่น จากนั้นนำมาเปรียบเทียบกับการวินิจฉัยขั้นสุดท้ายว่าก้อนนั้นเป็นเนื้องอกชนิดไม่ร้ายแรง หรือ มะเร็ง โดยอาศัยข้อมูลทางการแพทย์ทั้งหมด เช่นผลตรวจทางพยาธิวิทยา หรือ จากการวิเคราะห์ผลจากการติดตามการรักษาคน อ่าน 1 กรกฎาคม พ.ศ. 2545 ถึงวันที่ 30 มิถุนายน พ.ศ. 2546*

ผลการศึกษา: *ในผู้ป่วยทั้งหมด 64 คน มีก้อนที่ตับทั้งหมด 81 ก้อน ในจำนวนนี้การวินิจฉัยขั้นสุดท้ายที่สรุปว่าเป็นเนื้องอกชนิดไม่ร้ายแรงมี 62 ก้อน (ร้อยละ 76.5) เป็นมะเร็ง 19 ก้อน (ร้อยละ23.5) ในขณะที่การวินิจฉัยโดยคลื่นแม่เหล็กไฟฟ้า ให้การวินิจฉัยก้อนเหล่านี้เป็นเนื้องอกชนิดไม่ร้ายแรง 55 ก้อน เป็นมะเร็ง 17 ก้อน ไม่สามารถให้การวินิจฉัยได้ 9 ก้อน ถ้าหากรวมกลุ่มก้อนที่ไม่สามารถให้การวินิจฉัยได้เข้ากับกลุ่มที่เป็นเนื้องอกชนิดไม่ร้ายแรง ความไวและความจำเพาะมีค่าเท่ากับร้อยละ 68.4 และ 93.6 ตามลำดับ*

สรุป: *ในผู้ป่วยที่เอกซเรย์คอมพิวเตอร์ไม่สามารถให้การวินิจฉัยก้อนขนาดเล็กที่ตับ การตรวจด้วยเครื่องตรวจคลื่นแม่เหล็กไฟฟ้าจะสามารถช่วยให้การวินิจฉัยได้ด้วยความจำเพาะและความแม่นยำที่สูง*